

Note

The structural chemistry of triorganotin(IV) derivatives of 3-amino-5-mercapto-1,2,4-triazole: Supramolecular structures involving intermolecular N–H···N and N–H···S hydrogen bonding

Chunlin Ma ^{a,b,*}, Yongxin Li ^a, Yawen Han ^a, Rufen Zhang ^a^a Department of Chemistry, Liaocheng University, Liaocheng 252059, PR China^b Taishan University, Taian 271021, PR China

Received 1 June 2007; received in revised form 15 June 2007; accepted 15 June 2007

Available online 17 July 2007

Abstract

Four new triorganotin complexes of 3-amino-5-mercapto-1,2,4-triazole with the type of $R_3Sn(SC_2N_3HNH_2-3)$ ($R = Me$, **1**; n -Bu, **2**; Ph, **3**; $PhCH_2$, **4**) have been synthesized. All the complexes have been characterized by elemental analysis, IR, 1H NMR and ^{13}C NMR spectra. Complexes **1**, **3** and **4** have been characterized by X-ray crystallography analyses too. The geometry about Sn of complex **1** is distorted trigonal bipyramidal and the supramolecular structures of complex **1** has been found consist of channels built up by intermolecular N–H···N hydrogen bonding. The geometry of tin atoms in complexes **3** and **4** are distorted tetrahedron and 1D polymers connected by intermolecular N–H···N hydrogen bonding or N–H···N and N–H···S hydrogen bonding. Additionally, 1D polymer of complex **3** aggregated in 2D layer by intermolecular N–H···S hydrogen bonding.

© 2007 Elsevier B.V. All rights reserved.

Keywords: Triorganotin(IV); 3-Amino-5-mercapto-1,2,4-triazole; Hydrogen bonding

1. Introduction

Organotin complexes have been subjects of interest for some time because of their biological and commercial applications [1,2]. Increasing investigation of organotin(IV) complexes have been focused on acquiring well-defined solid-state structures to learn the nature of their versatile bonding modes [3], especially that of some organotin(IV) derivatives from heterocyclic thionates [4–7]. Heterocyclic thionates are ligands derived from heterocyclic thiones that contain at least one deprotonated heterocyclic thioamide group ($N-C-S$)[−] and can act as monodentate, chelating and bridging ligands. The aforementioned systems have been extensively studied in the field of coordination chem-

istry [8]. In our previous work, we studied the coordination chemistry of two ligands of such kind: 2-mercaptosuccinic (Hmnc) and 2,5-dimercapto-1,3,4-thiodiazole (HHdmt), which possess one and two deprotonated heterocyclic thioamide group ($N-C-S$)[−], respectively. The X-ray analyses revealed that the former acts in the thiol form, but the primary bond of the latter to the tin atom varies dramatically according to distinct R of the precursor R_nSnCl_{4-n} [9,10]. These results indicate there are several factors can influence the topologies of the organotin derivatives from heterocyclic thionates such as the special geometries of ligand, the special resistant from R of the precursor R_nSnCl_{4-n} , etc. To continue our study in this field, we chose another ligand: 3-amino-5-mercapto-1,2,4-triazole, which possesses one –SH and one –NH₂ group, through which primary bonds to tin atoms are likely formed. Moreover, the three potential coordination nitrogen atoms of triazole make the ligand act as a fulcrum about which lattice construction is orchestrated in one or more dimensions.

* Corresponding author. Address: Department of Chemistry, Liaocheng University, Liaocheng 252059, PR China. Tel.: +86 635 8230660; fax: +86 538 6715521.

E-mail address: macl@lcu.edu.cn (C. Ma).

In this paper, we report the syntheses, characterization and crystal structures of the related triorganotin derivatives **1–4**. All the complexes have been characterized by elemental analysis, IR, ^1H and ^{13}C NMR spectra. The geometry about Sn of complex **1** is distorted trigonal bipyramidal and the supramolecular structures of complex **1** has been found consist of 3D channels built up by intermolecular $\text{N–H}\cdots\text{N}$ hydrogen bonding. The geometry of tin atoms in complexes **3** and **4** are distorted tetrahedron and 1D polymers connected by intermolecular $\text{N–H}\cdots\text{N}$ hydrogen bonding or $\text{N–H}\cdots\text{N}$ and $\text{N–H}\cdots\text{S}$ hydrogen bonding.

2. Experimental

2.1. Materials and measurements

Trimethyltin chloride, tri-*n*-butyltin chloride, triphenyltin chloride, 3-amino-5-mercapto-1,2,4-triazole are commercially available, and they are used without further purification. Tribenzyltin chloride was prepared by a standard method reported in the literature [11]. The melting points were obtained with Kofler micro-melting point apparatus and were uncorrected. Infrared-spectra were recorded on a Nicolet-5700 spectrophotometer using KBr discs and sodium chloride optics. ^1H and ^{13}C NMR spectra were recorded on Varian Mercury Plus 400 spectrometer operating at 400 and 100.6 MHz, respectively. The spectra were acquired at room temperature (298 K) unless otherwise specified. ^{13}C spectra are broadband proton decoupled. The chemical shifts were reported in ppm with respect to the references and were stated relative to external tetramethylsilane (TMS) for ^1H and ^{13}C NMR. Elemental analyses were performed with a PE-2400II apparatus.

2.2. Syntheses of the complexes **1–4**

The reaction was carried out under nitrogen atmosphere with use of standard Schlenk techniques. The 3-amino-5-mercapto-1,2,4-triazole and the sodium ethoxide were added to the solution of benzene (20 ml), the mixture was stirred for 0.5 h. and then added triorganotin(IV) chloride to the mixture, continuing the reaction for 12 h at 40 °C. After cooling down to room temperature, filtered it. The solvent of the filtrate was gradually removed by evaporation under vacuum until solid product is obtained.

2.2.1. Synthesis of $(\text{CH}_3)_3\text{Sn}(\text{SC}_2\text{N}_3\text{HNH}_2-3)$ (**1**)

The colorless crystal complex **1** is formed from ethyl ether. Yield: 76%. m.p. 124–126 °C. Anal. Found: C, 21.41; H, 4.25; N, 19.90. Calc. for $\text{C}_5\text{H}_{12}\text{N}_4\text{SSn}$: C, 21.53; H, 4.34; N, 20.08%. IR (KBr, cm^{-1}): $\nu(\text{N–H})$ 3321, $\nu(\text{C=N})$ 1607, $\nu_{\text{as}}(\text{Sn–C})$ 530, $\nu_{\text{s}}(\text{Sn–C})$ 502, $\nu(\text{Sn–N})$ 496, $\nu(\text{Sn–S})$ 310. ^1H NMR (CDCl_3 , ppm): δ 0.73 (s, 9H, $^2J_{\text{SnH}} = 58$ Hz), δ 0.76 (s, 9H, Sn–CH_3), 4.81 (s, 2H, C–NH_2), 11.50 (s, H, N–H). ^{13}C NMR (CDCl_3 , ppm): δ 165.2 (C–S), 143.6 (C– NH_2), 8.09 (Me).

2.2.2. Synthesis of $(n\text{-Bu})_3\text{Sn}(\text{SC}_2\text{N}_3\text{HNH}_2-3)$ (**2**)

The solid is obtained from ethyl ether. Yield: 81%. m.p. 71–73 °C. Anal. Calc. for $\text{C}_{14}\text{H}_{30}\text{N}_4\text{SSn}$: C, 41.50; H, 7.46; N, 13.83. Found: C, 41.38; H, 7.34; N, 13.81%. IR (KBr, cm^{-1}): $\nu(\text{N–H})$ 3298, $\nu(\text{C=N})$ 1610, $\nu_{\text{as}}(\text{Sn–C})$ 528, $\nu_{\text{s}}(\text{Sn–C})$ 500, $\nu(\text{Sn–N})$ 483, $\nu(\text{Sn–S})$ 308. ^1H NMR (CDCl_3 , ppm): δ 0.85–1.71 (m, 27H, $\text{Sn–C}_4\text{H}_9$), 5.20 (s, 2H, C–NH_2), 11.41 (s, H, N–H). ^{13}C NMR (CDCl_3 , ppm): δ 165.3 (C–S), 143.2 (C– NH_2), 13.5, 26.3, 27.5, 29.2 (*n*-Bu).

2.2.3. Synthesis of $\text{Ph}_3\text{Sn}(\text{SC}_2\text{N}_3\text{HNH}_2-3)$ (**3**)

The solid is then recrystallized from ethyl ether and the white crystal complex **3** is formed. Yield: 88%. m.p. 182–184 °C. Anal. Calc. for $\text{C}_{20}\text{H}_{18}\text{N}_4\text{SSn}$: C, 51.64; H, 3.90; N, 12.04. Found: C, 51.51; H, 3.89; N, 11.88%. IR (KBr, cm^{-1}): $\nu(\text{N–H})$ 3305, $\nu(\text{C=N})$ 1598, $\nu_{\text{as}}(\text{Sn–C})$ 464, $\nu_{\text{s}}(\text{Sn–C})$ 429, $\nu(\text{Sn–N})$ 487, $\nu(\text{Sn–S})$ 311. ^1H NMR (CDCl_3 , ppm): δ 7.26–7.64 (m, 15H, $\text{Sn–C}_6\text{H}_5$), 5.00 (s, 2H, C–NH_2), 11.37 (s, H, N–H). ^{13}C NMR (CDCl_3 , ppm): δ 165.5 (C–S), 143.7 (C– NH_2), 127.9 (*m*-C), 129.3 (*p*-C), 136.5 (*o*-C), 148.3 (*i*-C).

2.2.4. Synthesis of $(\text{C}_6\text{H}_5\text{CH}_2)_3\text{Sn}(\text{SC}_2\text{N}_3\text{HNH}_2-3)$ (**4**)

The solid is then recrystallized from ethyl ether and the white crystal complex **4** is formed. Yield: 79%. m.p. 138–140 °C. Anal. Calc. for $\text{C}_{23}\text{H}_{24}\text{N}_4\text{SSn}$: C, 54.46; H, 4.77; N, 11.05. Found: C, 54.41; H, 4.62; N, 10.99%. IR (KBr, cm^{-1}): $\nu(\text{N–H})$ 3245, $\nu(\text{C=N})$ 1603, $\nu_{\text{as}}(\text{Sn–C})$ 450, $\nu_{\text{s}}(\text{Sn–C})$ 427, $\nu(\text{Sn–N})$ 483, $\nu(\text{Sn–S})$ 307. ^1H NMR (CDCl_3 , ppm): δ 3.51 (s, 6H, $\text{Sn–CH}_2\text{C}_6\text{H}_5$), 7.19–7.34 (s, 15H, $\text{Sn–CH}_2\text{C}_6\text{H}_5$), 5.09 (s, 2H, C–NH_2), 11.22 (s, H, N–H). ^{13}C NMR (CDCl_3 , ppm): δ 165.1 (C–S), 143.4 (C– NH_2), 37.5 ($\text{CH}_2\text{-Ph}$), 127.5 (*m*-C), 128.6 (*p*-C), 134.5 (*o*-C), 147.6 (*i*-C).

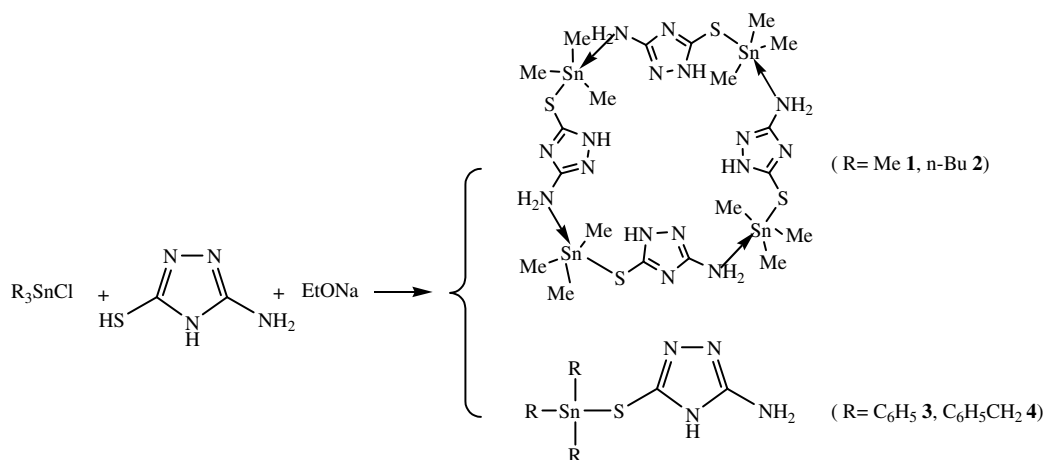
3. Results and discussion

3.1. Syntheses

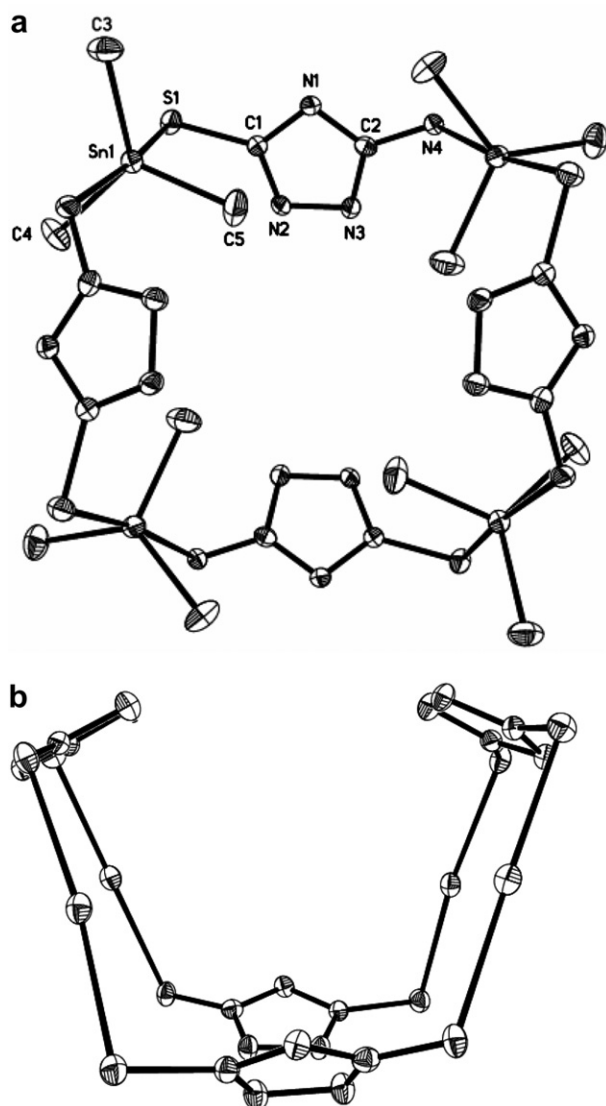
The synthesis procedure is shown in Scheme 1.

3.2. IR

The explicit feature in the infrared spectra of all complexes is the absence of the band in the region of 2558–2469 cm^{-1} , which appears in the free-ligand as $\nu(\text{S–H})$ vibration. For complexes **1–4**, the N–H stretching frequency reveal an upward shift 20–50 cm^{-1} relative to the frequency of the free ligand in the solids, which is indicative of the formation of an intermolecular $\text{N–H}\cdots\text{N}$ hydrogen bond. IR spectra appearing in the region 272–283 cm^{-1} are assigned to the Sn–S stretching mode of vibration, all of which are consistent with those detected in a number of organotin(IV)–sulfur complexes [12–14].



Scheme 1.



3.3. NMR

1H NMR data showed that the signal of the $-SH$ proton in the spectrum of the free ligand is absent in all of the complexes, demonstrating the removal of the $-SH$ proton and the formation of $Sn-S$ bonds. The ligand exhibits a single for the two protons of NH_2 in a very downfield region, indicating the intermolecular $N-H \cdots N$ hydrogen bonding, this is consistent with the IR spectra conclusion.

In the ^{13}C NMR spectra of all complexes, the chemical shifts of $C-S$ in complexes 1–4 are shifted by 11 ppm to low frequency compared with the free ligand (δ 176.2 ppm), indicating that the ligands involved in these complexes act as thiolate form.

3.4. Description of crystal structures of 1, 3 and 4

3.4.1. Crystal structure of $(CH_3)_3Sn(SC_2N_3HNH_2-3)$ (1)

The molecular structure of complex 1 is shown in Fig. 1a, selected bond lengths (\AA) and angles ($^\circ$) are listed in Table 1. Fig. 1 is viewed along c -axis, the structure is tetranuclear 24-membered macrocyclic structure (symmetry

Table 1
Selected bond lengths (\AA) and bond angles ($^\circ$) for complex 1

$Sn(1)-C(3)$	2.135(5)	$N(1)-C(1)$	1.339(5)
$Sn(1)-C(4)$	2.116(5)	$N(2)-C(1)$	1.330(5)
$Sn(1)-C(5)$	2.129(5)	$N(1)-C(2)$	1.347(5)
$Sn(1)-N(4)\#1$	2.697(4)	$S(1)-C(1)$	1.731(4)
$Sn(1)-S(1)$	2.608(1)	$N(3)-C(2)$	1.326(5)
$N(4)-C(2)$	1.391(5)		
$C(4)-Sn(1)-C(5)$	117.2(3)	$C(5)-Sn(1)-S(1)$	99.45(15)
$C(4)-Sn(1)-C(3)$	124.7(2)	$C(3)-Sn(1)-S(1)$	95.01(16)
$C(5)-Sn(1)-C(3)$	115.6(3)	$C(4)-Sn(1)-N(4)\#1$	83.73(16)
$C(4)-Sn(1)-S(1)$	91.45(15)	$C(5)-Sn(1)-N(4)\#1$	86.89(17)
$C(3)-Sn(1)-N(4)\#1$	83.87(17)	$S(1)-Sn(1)-N(4)\#1$	173.38(8)

Symmetry transformations used to generate equivalent atoms: $-y + 1/2$, x , $-z + 1/2$.

Fig. 1. (a) The molecular structure of complex 1 seen from c -axis. (b) The molecular structure of complex 1 seen from a -axis.

code: i: $-y + 1/2, x, -z + 1/2$; ii: $0.5 - x, 0.5 - y, z$). Trimethyltin moiety is bonded by the amino N atom and the deprotonated thiol S atom. The geometry about Sn is a distorted trigonal bipyramidal, with S and N occupied the axial position: S(1)–Sn(1)–N(4)#1 $173.37(8)^\circ$. The equatorial plane is occupied by three methyl groups and the sum of the angles around tin atom is $357.54(2)^\circ$, indicating that C(3), C(4), C(5) and Sn(1) are almost in a same plane with the slight deviation (mean deviation 0.0726 \AA). The Sn(1)–S(1) distance is $2.608(1) \text{ \AA}$, a little longer than the sum of the covalent radii of tin and sulfur (2.42 \AA) [15], but less than the sum of the van der Waal's radii of Sn and S atoms (4.0 \AA) [15], which proves that the sulfur atom is coordinated to the tin atom by a strong chemical bond. The Sn(1)–N(4)#1 distance ($2.699(4) \text{ \AA}$) is midway between the sum of the van der Waals and covalent radii of Sn and N (3.75 and 2.15 \AA , respectively) [16], but shorter than the corresponding Sn–N distances reported [17] in the literature and can be regarded as weak coordination bonds. If the molecular is viewed from *a*- or *b*-axis (Fig. 1b), it is much like a “boat” and can be valued through the transannular Sn \cdots Sn (6.592 \AA) distance. The N(1) and N(2) atoms are 4.016 \AA and 4.071 \AA from the Sn(1) atom, respectively, which is much longer than the sum of the van der Waal's

radii for Sn and N [15] and not indicative of a significant bonding interaction.

Furthermore, the adjacent “boat” can be connected together by intermolecular N2–H2 \cdots N3 ($\$1 -y + 1/2, x, -z - 1/2$) hydrogen bonding, so this structure gives rise to an interesting “pseudo-cage” and a channel is formed at the same time (Fig. 2). If observe the channel from the *c*-axis, a series of eight-membered rings parallel each other can be seen in Fig. 3 description. The width of 8-ring channel is $5.546(7) \times 5.452(7) \text{ \AA}$ (transannular N2 \cdots N3#1 #1: $0.5 - x, -0.5 + y, -z$). Furthermore, another intermolecular N–H \cdots N (N4–H4B \cdots N1 $\$3 (-x + 1, -y, -z)$) hydrogen bonding is found and link these channels together as can be seen from Fig. 3. At the same time another 20-member ring was formed due to the N4–H4B \cdots N1A hydrogen bonding (Fig. 3). Though the 22-member ring is larger than the eight-member ring, it is almost fully occupied by the methyl groups and the eight-member rings have a clearable “cavum” as can be seen from Fig. 4. The data of the hydrogen bonding are given in Table 4.

3.4.2. Crystal structures of $\text{Ph}_3\text{Sn}(\text{SC}_2\text{N}_3\text{HNNH}_2\text{-3})$ (3) and $(\text{C}_6\text{H}_5\text{CH}_2)_3\text{Sn}(\text{SC}_2\text{N}_3\text{HNNH}_2\text{-3})$ (4)

The molecular structures and the supramolecular structures are illustrated in Figs. 5–9, selected bond lengths (\AA)

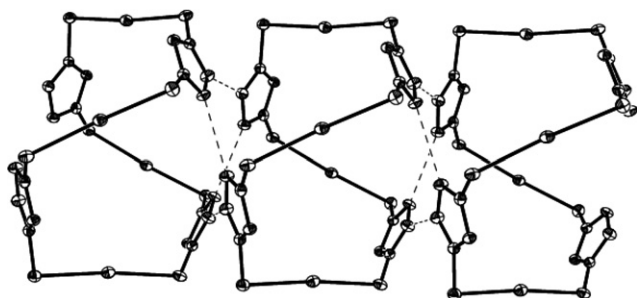


Fig. 2. The adjacent “boat” connected together by intermolecular N–H \cdots N hydrogen bonding of complex 1.

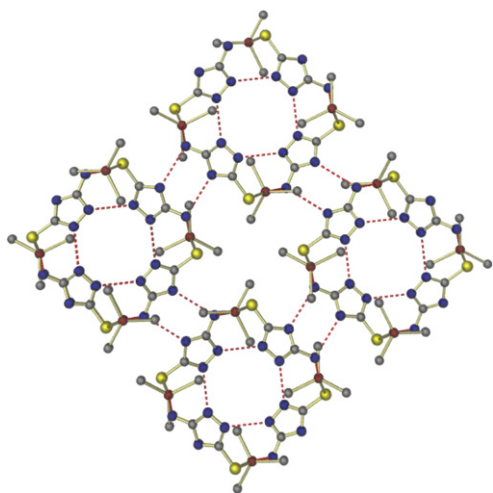


Fig. 3. The parallel channels connected together by intermolecular N–H \cdots N hydrogen bonding seen along the *c*-axis of complex 1.

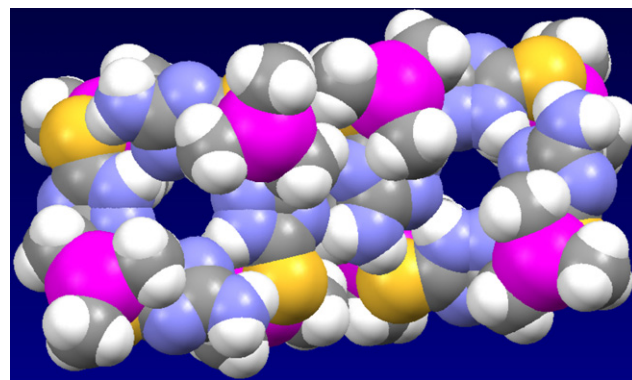


Fig. 4. The space-filling of complex 1, showing the “cavum” in this framework.

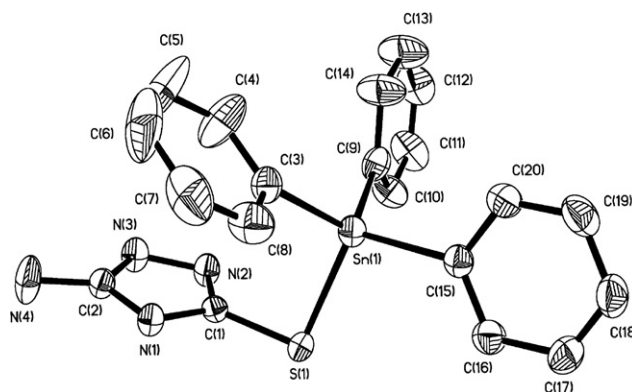


Fig. 5. The molecular structure of complex 3.

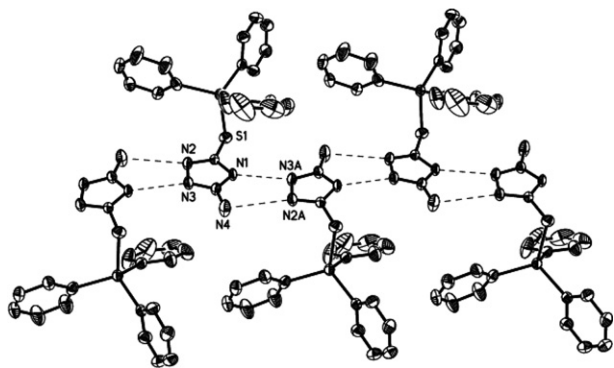


Fig. 6. 1D polymer connected by intermolecular N–H...N hydrogen bonding of complex **3**.

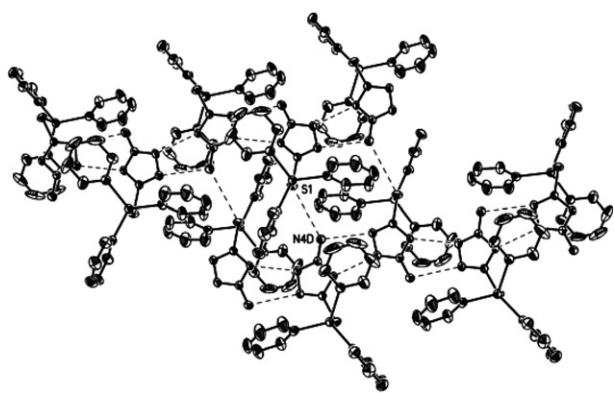


Fig. 7. 2D network of complex **3** connected by intermolecular N–H...N and N–H...S hydrogen bonding.

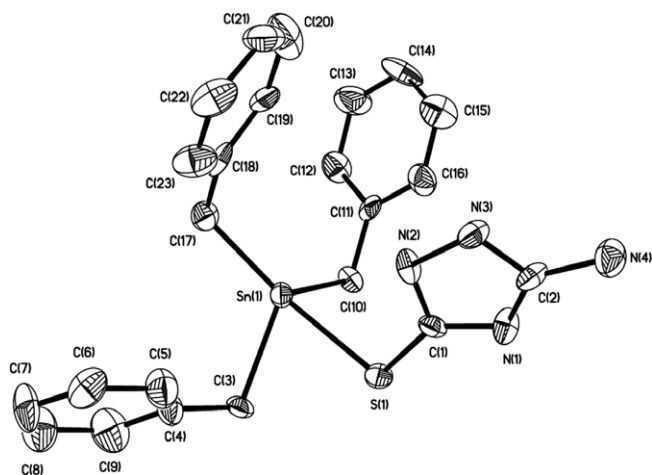


Fig. 8. The molecular structure of complex **4**.

and angles (°) are listed in Table 2. The geometry of the tin atoms involved four primary bonds: three to the phenyl (or benzyl) groups and one to sulfur atom. The Sn–S distances Sn(1)–S(1) 2.4223(17) Å for **3** and Sn(1)–S(1) 2.434(5) Å for **4** are falling in the Sn–S bond length range determined previously for triorganotin heteroarene thiolates (2.405–2.481 Å) [18,19] and approach the sum of the covalent radii of tin and sulfur (2.42 Å) [15], which proves that the sulfur

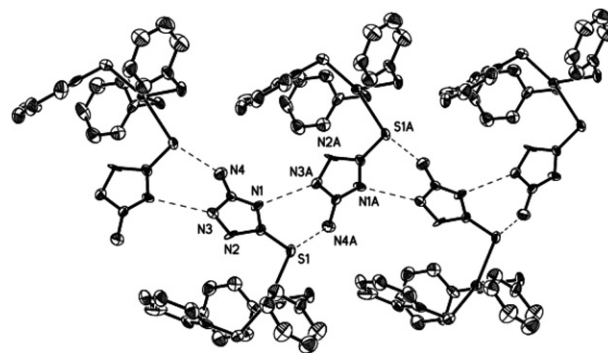


Fig. 9. 1D polymer of complex **4** connected by intermolecular N–H...N hydrogen bonding.

Table 2

Selected bond lengths (Å) and bond angles (°) for complexes **3** and **4**

Complex 3		Complex 4	
Sn(1)–C(3)	2.113(5)	Sn(1)–C(17)	2.102(18)
Sn(1)–C(15)	2.119(5)	Sn(1)–C(10)	2.250(13)
Sn(1)–C(9)	2.115(5)	Sn(1)–C(3)	2.249(15)
Sn(1)–S(1)	2.4223(17)	Sn(1)–S(1)	2.434(5)
Sn(1)–N(2)	3.651(4)	Sn(1)–N(2)	3.351(16)
C(3)–Sn(1)–C(9)	115.10(19)	C(17)–Sn(1)–C(3)	114.2(6)
C(3)–Sn(1)–C(15)	109.92(18)	C(10)–Sn(1)–C(3)	114.3(6)
C(9)–Sn(1)–C(15)	110.15(18)	C(17)–Sn(1)–C(10)	112.8(6)
C(3)–Sn(1)–S(1)	105.12(14)	C(3)–Sn(1)–S(1)	70.7(4)
C(9)–Sn(1)–S(1)	109.64(14)	C(17)–Sn(1)–S(1)	161.5(5)
C(15)–Sn(1)–S(1)	106.46(12)	C(10)–Sn(1)–S(1)	78.7(4)

atom is coordinated to the tin atom by a strong chemical bond. For complex **3**, the N(2) atom is 3.651(4) Å from the Sn(1) atom and much close to the sum of the van der Waal's radii for Sn and N [16], it is not indicative of a weak bonding interaction and the geometry of the tin atom is best described as distorted tetrahedron. This also can be confirmed by the angles around Sn(1) atom (105.12(14)–115.10(19)°), they are much close to the angles (109.5°) of ideal tetrahedron. Complex **4** is much different from the complex **3**, the N(2) atom is 3.351(16) Å from the Sn(1)

Table 3

Hydrogen bonding of complexes **1**, **3** and **4**

Complex	D–H...A	<i>d</i> (H...A) (Å)	∠DHA (°)	<i>d</i> (D...A) (Å)
1	N2–H2...N3A (\$1)	2.10	170.1	2.953 (5)
	N4–H4A...S1A(\$2)	2.82	138.2	3.511(4)
	N4–H4B...N1A(\$3)	2.33	150.3	3.106(5)
3	N1–H1...N3A ^a	2.03	154.8	2.833(5)
	N4–H4A...N2A ^b	2.30	153.7	3.097(6)
4	N4–H4B...S1A ^c	2.92	139.8	3.620(5)
	N1–H1...N3A (#1)	2.18	150.0	2.96(2)
	N4–H4B...S1A(#2)	2.87	123.3	3.416(19)

\$1 -y + 1/2, x, -z - 1/2; \$2 *y*, $-x + 1/2, -z - 1/2$; \$3 $-x + 1, -y, -z$.

#1 $-x - 1/2, y, z + 1/2$; #2 $-x - 1/2, y, z - 1/2$.

^a $-x + 1, y + 1/2, -z + 3/2$.

^b $-x + 1, y + 1/2, -z + 3/2$.

^c $x, -y + 1/2, z + 1/2$.

Table 4
Crystal data and structure refinement parameters for complexes **1**, **3** and **4**

Complex	1	3	4
Empirical formula	C ₅ H ₁₂ N ₄ SSn	C ₂₀ H ₁₈ N ₄ SSn	C ₂₃ H ₂₄ N ₄ SSn
Formula weight	278.94	465.13	507.21
Crystal system	tetragonal	monoclinic	orthorhombic
Space group	<i>P</i> 4 ₂ / <i>n</i>	<i>P</i> 2 ₁ / <i>c</i>	<i>Pca</i> 2 ₁
Unit cell dimension			
<i>a</i> (Å)	16.7143(17)	12.668(6)	13.819(11)
<i>b</i> (Å)	16.7143(17)	9.577(4)	16.748(13)
<i>c</i> (Å)	7.2782(15)	16.596(8)	9.803(7)
β (°)	90	89.500(7)	90
Flack parameter			0.29(8)
<i>Z</i>	8	4	4
Absorption coefficient (mm ^{−1})	2.670	1.383	1.485
Crystal size (mm)	0.42 × 0.31 × 0.27	0.42 × 0.36 × 0.23	0.55 × 0.48 × 0.42
θ Range for data collection (°)	2.44–24.99	2.46–25.12	1.91–25.02
Reflections collected (<i>R</i> _{int})	10279	9575	10116
Unique reflections	1798 (0.0563)	3379 (0.0405)	3267 (0.1557)
Data/restraint/parameters	1798/0/100	3379/0/235	3267/43/262
Goodness-of-fit on <i>F</i> ²	1.007	1.001	1.009
Final <i>R</i> indices [<i>I</i> > 2 σ (<i>I</i>)]	<i>R</i> ₁ = 0.0303, <i>wR</i> ₂ = 0.0749	<i>R</i> ₁ = 0.0381, <i>wR</i> ₂ = 0.0873	<i>R</i> ₁ = 0.0729, <i>wR</i> ₂ = 0.1815
<i>R</i> indices (all data)	<i>R</i> ₁ = 0.0456, <i>wR</i> ₂ = 0.0862	<i>R</i> ₁ = 0.0561, <i>wR</i> ₂ = 0.0958	<i>R</i> ₁ = 0.0942, <i>wR</i> ₂ = 0.2102

atom and much shorter than the sum of the van der Waal's radii for Sn and N [16], it is can be considered as an weak intermolecular interaction. This also can be confirmed by the angles around Sn atom, the angles are range from 70.7(4)° to 161.5(5)° and completely deviation from the ideal tetrahedron structure. As the N(2) atom is involved in a weak coordinative interaction with tin along one of the tetrahedral faces, the structure distortion for the tin atom in complex **4** is best described as capped distorted tetrahedron.

The supramolecular structure of **3** consists of a 1D chains in which adjacent molecular are assembled by N–H···N hydrogen bonding as can be seen from Fig. 6. Furthermore, these chains interconnect each other through intermolecular N4–H4B···S1 (2.92 Å, 3.620(5) Å, 139.8°) hydrogen bonding, resulting in an expanded 2D layer. Though the H···S distance is much weaker than the previous reported (2.32–2.693 Å) [20–22], it govern the assembly of the molecules in the 2D architecture (Fig. 8). Complex **4**

is similar to the complex **3**, 1D polymer was formed by intermolecular N1–H1···N3A and N4–H4B···S1 hydrogen bonding as can be seen from Fig. 9. The data are list in Table 3, all these data are close to that in complex **3**.

4. X-ray crystallography

All X-ray crystallographic data were collected on a Bruker SMART CCD 1000 diffractometer with graphite-monochromated Mo K α radiation (λ = 0.71073 Å) at 298(2) K. A semi-empirical absorption correction was applied to the data. The structure was solved by direct methods using SHELXS-97 and refined against *F*² by full-matrix least-squares using SHELXL-97. Hydrogen atoms were placed in calculated positions. Crystal data and experimental details of the structure determinations are list in Table 4.

Acknowledgement

We thank the National Natural Science Foundation of China (20271025) for financial support.

Appendix A. Supplementary material

CCDC 285726, 220172 and 235030 contain the supplementary crystallographic data (excluding structure factors) for **1**, **3** and **4**. These data can be obtained free of charge via <http://www.ccdc.cam.ac.uk/conts/retrieving.html>, or from the Cambridge Crystallographic Data Centre, 12 Union Road, Cambridge CB2 1EZ, UK; fax: (+44) 1223-336-033; or e-mail: deposit@ccdc.cam.ac.uk. Supplementary data associated with this article can be found, in the online version, at doi:10.1016/j.ica.2007.06.045.

References

- [1] T.S.B. Basu, S. Dhar, S.M. Pyke, E.R.T. Tiekink, E. Rivarola, R. Butcher, F.E. Smith, J. Organomet. Chem. 633 (2001) 7.
- [2] M. Kemmer, H. Dalil, M. Biesemans, J.C. Martins, B. Mahieu, E. Horn, D. de Vos, E.R. T. Tiekink, R. Willem, M. Gielen, J. Organomet. Chem. 608 (2000) 63.
- [3] M. Suzuki, H. Son, R. Noyori, H. Masuda, Organometallics 9 (1990) 3043.
- [4] J.A. Deiters, R.R. Holmes, J. Chem. Soc., Dalton Trans. (1988) 1259.
- [5] K.C. Molly, S.J. Blunder, R. Hill, J. Chem. Soc., Dalton Trans. (1988) 1259.
- [6] S. Bhandari, M.F. Mahon, J.G. McGinley, K.C. Molly, C.E.E. Roper, J. Chem. Soc., Dalton Trans. 20 (1998) 3425.
- [7] R. Cea-Olivares, O.J. Sandoval, G. Espinosa-Perez, C. Silvestru, Polyhedron 13 (1994) 809.
- [8] E.S. Raper, Coord. Chem. Rev. 153 (1996) 199.
- [9] C.L. Ma, F. Li, Q. Jiang, R.F. Zhang, J. Organomet. Chem. 689 (2004) 96.
- [10] C.L. Ma, Q. Jiang, R.F. Zhang, J. Organomet. Chem. 678 (2003) 148.
- [11] K. Sisido, Y. Takeda, Z. Kinugawa, J. Am. Chem. Soc. 83 (1961) 538.
- [12] C.V. Rodarte de Moura, A.P.G. de Sousa, R.M. Silva, A. Abras, M. Hörner, A.J. Bortoluzzi, C.A.L. Filgueiras, J.L. Wardell, Polyhedron 18 (1999) 2961.

- [13] A.P.G. de Sousa, R.M. Silva, A. Cesar, J.L. Wardell, J.C. Huffman, A. Abras, *J. Organomet. Chem.* 605 (2000) 82.
- [14] J.S. Casas, E.G. Martinez, J. Sordo, M.L. Jorge, U. Russo, *Appl. Organomet. Chem.* 15 (2001) 204.
- [15] A. Bondi, *J. Phys. Chem.* 68 (1964) 441.
- [16] T. Schoop, H.W. Roesky, M. Noltemeyer, H.G. Schmidt, *Organometallics* 12 (1993) 571.
- [17] J.E. Huheey, *Inorganic Chemistry: Principles of Structure and Reactivity*, third ed., Harper International, New York, 1983, p. 258.
- [18] J.S. Casas, A. Castineiras, E.G. Martinez, A.S. González, A. Sánchez, J. Sordo, *Polyhedron* 16 (1997) 795.
- [19] B.D. James, R.J. Magee, W.C. Patalinghug, B.W. Skelton, A.H. White, *J. Organomet. Chem.* 476 (1994) 51.
- [20] V. Berceanc, C. Crainic, I. Haiduc, M.F. Mahon, K.C. Molly, M.M. Venter, P.J. Wilson, *J. Chem. Soc., Dalton Trans.* (2002) 1036.
- [21] V.R. Pedireddi, S. Chatterjee, A. Ranganathan, C.N.R. Rao, *J. Am. Chem. Soc.* 119 (1997) 10867.
- [22] A. Ranganathan, V.R. Pedireddi, C.N.R. Rao, *J. Am. Chem. Soc.* 121 (1999) 752.